Pulsed-beam propagation in lossless dispersive media. I. Theory

Timor Melamed and Leopold B. Felsen*

Department of Aerospace and Mechanical Engineering, Boston University, 110 Cummington Street, Boston, Massachusetts 02215

Received September 2, 1997; accepted December 2, 1997; revised manuscript received January 15, 1998

This first part of a two-part investigation is concerned with the effects of dispersion on the propagation characteristics of the scalar field associated with a highly localized pulsed-beam (PB) wave packet in a lossless homogeneous medium described by the generic wave-number profile $k(\omega) = \omega/c(\omega)$, where $c(\omega)$ is the frequency-dependent wave propagation speed. While comprehensive studies have been performed for the one-dimensional problem of pulsed plane-wave propagation in dispersive media, particularly for specific $c(\omega)$ profiles of the Lorentz or Debye type, even relatively crude measures tied to generic $k(\omega)$ profiles do not appear to have been obtained for the three-dimensional problem associated with a PB wave packet with complex frequency and wave-number spectral constituents. Such wave packets have been well explored in nondispersive media, and simple asymptotic expressions have been obtained in the paraxial range surrounding the beam axis. These paraxially approximated wave objects are now used to formulate the initial conditions for the lossless generic $k(\omega)$ dispersive case. The resulting frequency inversion integral is reduced by simple saddle-point asymptotics to extract the PB phenomenology in the well-developed dispersive regime. The phenomenology of the transient field is parameterized in terms of the space–time evolution of the PB wave-front curvature, spatial and temporal beam width, etc., as well as in terms of the corresponding space–time-dependent frequencies of the signal, which are related to the local geometrical properties of the $k(\omega)$ dispersion surface. These individual parameters are then combined to form nondimensional critical parameters that quantify the effect of dispersion within the space–time range of validity of the paraxial PB. One does this by performing higher-order asymptotic expansions beyond the paraxial range and then ascertaining the conditions for which the higher-order terms can be neglected. In Part II [J. Opt. Soc. Am. A **15**, 1276 (1998)], these studies are extended to include the transitional regime at those early observation times for which dispersion is not yet fully developed. Also included in Part II are analytical and numerical results for a simple Lorentz model that permit assessment of the performance of various nondimensional critical estimators. © 1998 Optical Society of America [S0740-3232(98)02805-1]

OCIS codes: 260.2030, 050.1940, 270.5530, 350.5500.

1. INTRODUCTION

Time-domain (TD) signal interaction with lossy dispersive materials is an important problem area that has attracted the attention of analysts since the beginning of this century. Even the one-dimensional problem of pulsed-plane-wave propagation in such media, when explored in detail, contains a wealth of subtleties in phenomenology that can be parameterized by carrying out sophisticated asymptotic evaluations of the spectral integrals that result when the frequency-domain (FD) solutions are Fourier inverted into the TD.[1] For a comprehensive treatment, see Refs. 2–6. There have been much fewer, and less comprehensive, corresponding studies of the three-dimensional problem posed by more realistic space–time-limited initial conditions. The present investigation is concerned with the parameterization of general transient fields in terms of localized pulsed-beam (PB) wave packets that, when defined as analytic signals in complex space–time, possess the following desirable properties: 1. The PB's form a complete basis for decomposition and synthesis of actual space–time-dependent fields.[7,8] 2. The PB's are highly localized propagators whose progress in the configuration (space–time) domain, as well as in the spectrum (wave-number–frequency) domain, can be tracked analytically.[8–10] 3. The PB initial conditions are space–time Gaussian window functions that can be used for physically based preprocessing and postprocessing of space–time input and output data; this property is relevant for high-resolution dynamic imaging.[11–13] 4. The PB's are isodiffracting, which means that all their frequency components have the same collimation length and wave-front radius of curvature.[14] The FD analytic signal analogs of the PB are beams generated by time-harmonic sources in complex space. They possess the same completeness, etc., properties as the PB and can be employed for characterization of FD portions of the TD problem.

In this two-part sequence we treat the evolution of the signal excited by PB initial conditions in a lossless homogeneous dispersive medium described generically by the frequency-dependent wave number $k(\omega)$. As for the plane-wave case, this requires asymptotic analysis of the Fourier inversion integral from the FD. However, unlike the plane-wave case, the PB input also requires spectral analysis and synthesis in the wave-number domain. This has already been performed in previous studies[8] with emphasis on paraxial asymptotics for approximating the PB propagators. We shall employ this useful approximation in the inversion integral from the FD. Our goal is to extract, by using simple high-frequency saddle-

0740-3232/98/051268-09$15.00

point asymptotics, the effects of dispersion on the paraxial PB propagators. These effects will be characterized and quantified in terms of critical nondimensional parameters that capture the relevant wave physics pertaining to various space–time observation domains for various choices of PB spatial widths D and pulse lengths T. In the well-developed dispersive regime, this can be done for the generic $k(\omega)$. The critical nondimensional descriptors, i.e., the footprints, of various observables of the paraxial PB-excited signal, are calibrated through higher-order off-axis expansions beyond the second-order paraxial range, thereby allowing quantitative limits to be established by examination of the conditions for neglecting the higher-order terms. Because the PB spectra contain complex frequencies and wave numbers, many alternative options for off-axis exploration are available, with different associated wave physics. The space–time-dependent saddle-point frequency $\omega_s(\mathbf{r}, t)$, where ω_s is complex, and the space–time envelope $E(\mathbf{r}, t)$ of the signal play a central role in these explorations.

It is known that space–time wave asymptotics in dispersive media can be interpreted graphically in terms of space–time ray theory and the simultaneous use of the wave-number–frequency dispersion surfaces. In general, this visualization involves the four-dimensional complex (space–time)–(wave-number–frequency) phase space. For asymptotic wave processes described by real spectra in lossless dispersive media, the phase space is real, and its utilization can be found, for example, in Ref. 15. The wave dynamics are closely tied to the radius of curvature R_c of the dispersion surface and to the radius of curvature R of the incident signal wave front. These parameterizations are utilized and extended in the present treatment to account for the complex spectra associated with the paraxial PB. Accordingly, R and R_c appear in the nondimensional measures that quantify the corrections attributed to the complex spectra in the PB.

The layout of this two-part sequence is as follows. The present paper, Part I, addresses the fully dispersive asymptotic regime for a generic $k(\omega)$ dispersion relation. The statement of the problem is given in Section 2. Wave-number analysis and synthesis in the FD, followed by asymptotic evaluation, is given in Section 3. Inversion from the FD to the TD and the associated asymptotics is presented in Section 4. Two basic cases are treated there depending on the spectral amplitude $\hat{f}(\omega)$: 1. $\hat{f}(\omega)$ treated as an amplitude, 2. $\hat{f}(\omega)$ incorporated into the phase. Case 2 pertains to the PB input and occupies the major portion of this section. Defined and quantified here are various measures of the effect of dispersion on the PB signal. Conclusions are given in Section 5.

The companion paper, Part II,[16] treats the transition regions, close to the wave front, where the high frequencies in the pulse spectrum predominate and where full dispersion has not yet been established. Here it is necessary to resort to a specific model of $k(\omega)$. Our specific model is for a lossless Lorentz-type medium,[2] and a closed-form transition function is developed that traces the evolution from the nondispersed regime very near the wave front to the fully dispersed regime sufficiently far behind the wave front. Also included there for the same medium are calculations of the various asymptotic measures developed in the present paper and comparisons with numerical reference data to assess their validity and accuracy.

2. STATEMENT OF THE PROBLEM

The problem of PB wave-packet propagation in a lossless, homogeneous, isotropic dispersive medium is defined by the PB-matched initial distribution in the FD and is Fourier inverted from there into the TD. The time–frequency and space–(wave-number) transform relations required for implementation are listed in Subsections 2.A and 2.B, respectively, and the FD initial distribution for generalizing the PB is given in Subsection 2.C.

A. Time–Frequency Transforms

Given a TD field, $u(\mathbf{r}, t)$, the corresponding FD field $\hat{u}(\mathbf{r}; \omega)$ is defined by the Fourier-transform relations

$$\hat{u}(\mathbf{r}, \omega) = \int_{-\infty}^{\infty} u(\mathbf{r}, t)\exp(i\omega t)\mathrm{d}t, \tag{1a}$$

$$u(\mathbf{r}, t) = \frac{1}{2\pi}\int_{-\infty}^{\infty} \hat{u}(\mathbf{r}, \omega)\exp(-i\omega t)\mathrm{d}\omega, \tag{1b}$$

where $\mathbf{r} = (x_1, x_2, z)$ are conventional Cartesian coordinates. Here, and henceforth, FD fields are denoted by a caret ($\hat{}$) above the variable. Throughout, we shall utilize the analytic signal formulation for time-dependent fields to accommodate wave constituents with evanescent (i.e., complex) spectra, as encountered in the PB. The analytic field $\overset{+}{u}(\mathbf{r}, t)$ (denoted by a plus sign above the variable) corresponding to the FD field $\hat{u}(\mathbf{r}, \omega)$ is obtained by the one-sided Fourier inverse transform

$$\overset{+}{u}(\mathbf{r}, t) = \frac{1}{\pi}\int_{0}^{\infty} \hat{u}(\mathbf{r}, \omega)\exp(-i\omega t)\mathrm{d}\omega, \qquad \mathrm{Im}\, t \leqslant 0, \tag{2}$$

where $\hat{u}(\mathbf{r}, \omega)$ is defined as in Eq. (1a). The real field is obtained in this formulation from the real part of the analytic field:

$$u(\mathbf{r}, t) = \mathrm{Re}\, \overset{+}{u}(\mathbf{r}, t). \tag{3}$$

B. Space–(Wave-Number) Transforms

As noted above, the TD initial distribution $u_0(\mathbf{x}, t)$ for the PB on the $z = 0$ plane will be synthesized via inversion of the corresponding FD distribution $\hat{u}_0(\mathbf{x}, \omega)$. The FD wave-number spectral amplitude on the initial surface is given by

$$\tilde{\hat{u}}_0(\boldsymbol{\xi}, \omega) = \int_{-\infty}^{\infty} \mathrm{d}^2x\, \hat{u}_0(\mathbf{x}, \omega)\exp[-ik(\omega)\boldsymbol{\xi}\cdot\mathbf{x}], \tag{4a}$$

where $\boldsymbol{\xi} = (\xi_1, \xi_2)$ is the normalized spatial wave-number vector; $\mathbf{x} = (x_1, x_2)$; $k(\omega)$ is the frequency-dependent wave number in the ambient medium; and $\tilde{}$ identifies a wave-number spectral function. The reconstruction of the FD initial field is, accordingly,

$$\hat{u}_0(\mathbf{x}, \omega) = [k(\omega)/2\pi]^2 \int \mathrm{d}^2\xi\, \tilde{\hat{u}}_0(\boldsymbol{\xi}, \omega)\exp[ik(\omega)\boldsymbol{\xi}\cdot\mathbf{x}]. \tag{4b}$$

The normalization with respect to the wave number $k(\omega)$ anticipates inversion to the TD, rendering ξ frequency independent, with direct geometrical interpretation in terms of the spectral plane-wave propagation angles. For simplicity, the ω dependence of $k = k(\omega)$ and of $\hat{u}(\mathbf{r}) = \hat{u}(\mathbf{r}, \omega)$ shall be suppressed unless specifically required for clarity. Also, integration limits are omitted on all integrals extending from $-\infty$ to $+\infty$.

By inclusion of the plane-wave spectral propagator $\exp(ik\zeta z)$, the plane-wave representation for the FD field away from the initial plane is

$$\hat{u}(\mathbf{r}, \omega) = (k/2\pi)^2 \int \mathrm{d}^2\xi \hat{\tilde{u}}_0(\boldsymbol{\xi}) \exp[ik(\boldsymbol{\xi} \cdot \mathbf{x} + \zeta z)], \tag{5}$$

where

$$\zeta = \sqrt{1 - \xi^2}, \qquad \xi^2 \equiv \boldsymbol{\xi} \cdot \boldsymbol{\xi}, \qquad \mathrm{Im}\, \zeta \geqslant 0. \tag{6}$$

Inserting Eq. (5) into Eq. (2), we obtain the formal plane-wave spectral representation of the TD analytic field at any observation point $\mathbf{r}$:

$$\overset{+}{u}(\mathbf{r}, t) = \frac{1}{\pi} \int_0^\infty \mathrm{d}\omega \left[\frac{k(\omega)}{2\pi}\right]^2 \int \mathrm{d}^2\xi \hat{\tilde{u}}_0(\boldsymbol{\xi}, \omega) \times \exp[-i\omega t + ik(\omega)(\boldsymbol{\xi} \cdot \mathbf{x} + \zeta z)]. \tag{7}$$

C. Initial Distribution

The initial field distribution is chosen so that it generates a PB wave packet in the dispersive environment. For purposes of focusing such a wave packet at a particular space–time point, it is desirable to select the beam parameters in such a way that the focusing distance is independent of frequency. In the FD such isodiffracting initial distributions have the form[14]

$$\hat{u}_0(\mathbf{x}, \omega) = \hat{f}(\omega) \exp[-(1/2)k(\omega)\rho^2/\beta], \tag{8}$$

where $\rho^2 \equiv \mathbf{x} \cdot \mathbf{x}$, $\hat{f}$ is some frequency-dependent function, and $\beta = \beta_r + i\beta_i$ (with $\beta_r > 0$ for $\omega > 0$) is a frequency-independent parameter. The corresponding plane-wave spectrum $\hat{\tilde{u}}_0$ of the above distribution, obtained by inserting Eq. (8) into Eq. (4a), is

$$\hat{\tilde{u}}_0(\boldsymbol{\xi}, \omega) = (2\pi \hat{f}\beta/k) \exp[-(1/2)k\beta\xi^2]. \tag{9}$$

The TD initial distribution is obtained via the Fourier inversion in Eq. (2), yielding $u_0(\mathbf{x}, t) = \mathrm{Re}\, \overset{+}{u}_0(\mathbf{x}, t)$, with

$$\overset{+}{u}_0(\mathbf{x}, t) = \int_0^\infty \mathrm{d}\omega \hat{f}(\omega) \exp\left[-i\omega t - \frac{1}{2} k(\omega)\rho^2/\beta\right]. \tag{10}$$

Note that the integral in Eq. (10) depends on the details of the dispersive medium, which is thus far described by the generic dispersion relation $k = k(\omega)$.

In evaluating the integral given in Eq. (7), two approaches may be considered: (1) FD first, in which one evaluates the FD field by $\mathrm{d}^2\xi$ integration before transforming the result into the TD with Eq. (1a); and (2) TD first, which involves interchanging the order of integration in Eq. (7) and evaluating the $\mathrm{d}\omega$ integral first, thereby yielding a transient plane-wave spectral representation for the field in the dispersive medium. The second approach is the subject of a separate discussion and is not included here.

3. FREQUENCY-DOMAIN SPECTRAL INTEGRAL AND PARAXIAL ASYMPTOTICS

The FD field, corresponding to the FD initial distribution in Eq. (8), is given by the plane-wave spectral integral in Eq. (5):

$$\hat{u}(\mathbf{r}, \omega) = [\beta k(\omega)\hat{f}(\omega)/2\pi] \int \mathrm{d}^2\xi \exp\left[-i\omega t + ik(\omega) \times \left(\frac{i}{2}\beta\xi^2 + \boldsymbol{\xi} \cdot \mathbf{x} + \zeta z\right)\right]. \tag{11}$$

Using the saddle-point technique, as well as a paraxial approximation, we can evaluate this integral asymptotically. The result is[8]

$$\hat{u}(\mathbf{r}, \omega) \sim \hat{f}(\omega) \frac{-i\beta}{z - i\beta} \exp[ik(\omega)S(\mathbf{r})], \tag{12}$$

where

$$S(\mathbf{r}) = z + {}^1\!/_2\rho^2/(z - i\beta) \tag{13}$$

is the normalized paraxial phase.

From relation (12) with Eq. (13), the field is identified as a paraxial Gaussian beam (GB) propagating in the z direction. To parameterize the beam field, we write the real and the imaginary parts of S as follows:

$$S = z + {}^1\!/_2\rho^2/(z - Z - iF) = z + {}^1\!/_2\rho^2(1/R + i/I), \qquad I = kD^2, \tag{14}$$

where

$$Z = -\beta_i, \qquad F = \beta_r, \tag{15}$$

$$D = \sqrt{F/k}[1 + (z - Z)^2/F^2]^{1/2}, \tag{16}$$

$$R = (z - Z) + F^2/(z - Z). \tag{17}$$

By substituting Eq. (14) into relation (12) one readily identifies $2\sqrt{2}D$ and R as the $1/e$ beam width and the phase-front radius of curvature, respectively. The GB waist is located at $z = Z$, and its collimation length is F. Note that the waist location Z, the collimation length F, and therefore I as well as the phase S as a whole are frequency independent, as intended. However, the beam width D is frequency dependent, being proportional to $k^{-1/2}$.

4. TIME-DOMAIN INVERSION AND PARAXIAL ASYMPTOTICS

The TD representation for the PB field, corresponding to the asymptotic (paraxial) FD field in relation (12), is obtained by the one-sided Fourier inversion in Eq. (2), i.e.,

$$\overset{+}{u}(\mathbf{r}, t) = \frac{-i\beta}{z - i\beta}\frac{1}{\pi}\int_0^\infty d\omega\ \hat{f}(\omega)\exp[-i\Phi(\omega; \mathbf{r}, t)], \tag{18}$$

$$\Phi(\omega; \mathbf{r}, t) = \omega t - k(\omega)S(\mathbf{r}), \tag{18a}$$

where S is defined as in Eq. (13).

A. Nondispersive Case

For nondispersive media, the integral in Eqs. (18) can be evaluated in closed form. Inserting $k(\omega) = \omega/c$ into Eq. (18), we obtain $u(\mathbf{r}, t) = \mathrm{Re}\ \overset{+}{u}(\mathbf{r}, t)$, where

$$\overset{+}{u}(\mathbf{r}, t) = \frac{-i\beta}{z - i\beta}\overset{+}{f}\left\{t - c^{-1}\left[z + \frac{1}{2}\rho^2/(z - i\beta)\right]\right\}. \tag{19}$$

One can obtain a conventional waveform by choosing[8]

$$\hat{f}(\omega) = \exp(-\omega T/2), \tag{20}$$

which implies that

$$\overset{+}{f}(t) = \overset{+}{\delta}(t - iT/2), \qquad f(t) = \mathrm{Re}\ \overset{+}{f} = \frac{1}{\pi}\frac{T/2}{t^2 + (T/2)^2}, \tag{20a}$$

where $\overset{+}{\delta}(t) = 1/\pi i t$ is the analytic δ function defined in the lower half of the complex t plane. This waveform peaks at $t = 0$, and its pulse length and peak values are given by T and $2/\pi T$, respectively. Also note that the maximum frequency of this signal may be estimated by

$$\omega_{\max} \simeq T^{-1}. \tag{21}$$

Therefore such a band-limited pulse may be regarded as a model for a physical (sampled) signal. Inserting Eq. (20a) into Eq. (19), we obtain

$$\overset{+}{u}(\mathbf{r}, t) = \frac{-i\beta}{z - i\beta}\overset{+}{\delta}\left\{t - i\frac{T}{2} - c^{-1}\left[z + \frac{1}{2}\rho^2/(z - i\beta)\right]\right\}. \tag{22}$$

This PB field has been discussed thoroughly in Refs. 8–10. Here we summarize the main features, since they are also relevant for the dispersive case. The PB field in Eq. (22) propagates along the z axis. Its space–time structure may be inferred from the elements of the frequency-independent normalized phase S in Eq. (14), with $R(z)$ in Eq. (17) now being interpreted as the wave-front radius of curvature and $T_p(\mathbf{r}) = T + c^{-1}\rho^2/I(z)$ being interpreted as the temporal half-amplitude width of the $\overset{+}{\delta}$ pulse, which is inversely proportional to the pulse amplitude [see $f(t)$ in Eqs. (20a)]. The field is strongest on the beam axis $\rho = 0$, where $T_p(\mathbf{r}) = T$ is minimal, and it decays as T_p grows away from the beam axis. On the wave front, $t = c^{-1}[z + \rho^2/2R(z)]$, the field amplitude is proportional to ${T_p}^{-1}(\rho)$, and one finds the half-amplitude beam width in the ρ direction by solving $T_p(\rho) = 2T_p(0)$, giving

$$D(z) = 2\sqrt{cTI(z)}. \tag{23}$$

The collimation length is given by F in Eqs. (15), and the waist is located at $z = Z$ with the width $2\sqrt{cTF}$. From Eq. (23) with Eq. (14) one notes that, in the collimation (Fresnel) zone $|z - Z| < F$, the PB profile is essentially unchanged, whereas outside this zone the profile broadens and approaches the asymptotic far-field diffraction angle

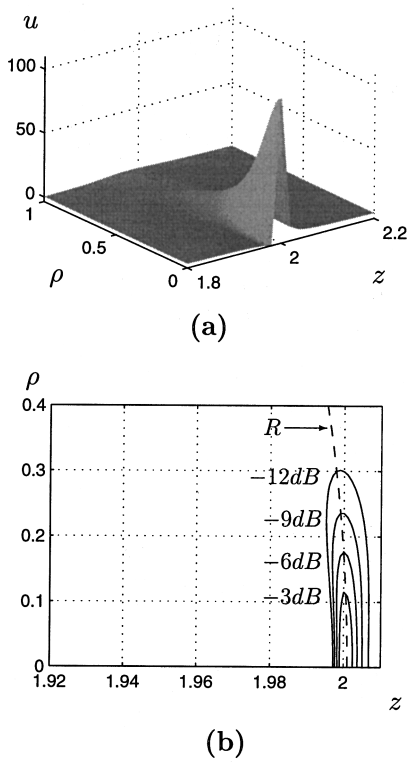

Fig. 1. Nondispersive PB field [Eq. (22)] for $cT = 0.005$, $\beta = 5$, $ct = 2$. At the wave front $z = ct = 2$, this set of parameters yields a spatial beam width $D/2 = 0.16$ in Eq. (23), a wave-front radius of curvature $R = 14.5$, and a temporal on-axis width $T_p(0) = T = 0.005$. (a) u versus (ρ, z); (b) (ρ, z) contour plot.

$$\Theta = 2\sqrt{cT/F}. \tag{24}$$

A snapshot of the nondispersive PB field [Eq. (22)] is presented in Fig. 1 for $T = 0.005$, $\beta = 5$, $ct = 2$. At $z = ct$, this set of parameters yields a spatial beam width $D/2 = 0.16$ in Eq. (23), a wave-front radius of curvature $R = 14.5$, and a temporal on-axis width $T_p(0) = T = 0.005$.

In summary, the propagator in Eq. (22) belongs to the class of isodiffracting[14] PB fields whose frequency components all have the same collimation distance and radius of curvature.

B. Dispersive Case

When the medium is dispersive, the integral in Eqs. (18) cannot generally be evaluated in closed form. We shall evaluate Eqs. (18) asymptotically by continuing the integrand in Eqs. (18) analytically into the complex ω plane and applying the saddle-point method, with the saddle point being denoted by ω_s. Our goal is the parameterization of the effect of dispersion on the paraxial PB field. To quantify the effect, it is necessary to retain higher-order terms in the transverse coordinate ρ at various stages of the analysis. Accordingly, when necessary, paraxial $O(\rho^2)$ quantities shall be identified by the subscript p.

1. $\hat{f}(\omega)$ Treated as an Amplitude

We assume first that $\hat{f}$ is an amplitude function without ω-dependent phase. Setting the first derivative of the phase Φ in Eq. (18a) to zero, we obtain

$$\frac{t}{S(\mathbf{r})} = \left.\frac{\mathrm{d}k}{\mathrm{d}\omega}\right|_{\omega_s}. \tag{25}$$

a. On-Axis Field. Instead of solving Eq. (25) formally, we utilize the spatial localization of the Gaussian beam in relation (12) and examine the paraxial region around the beam axis. Note that, for $\rho = 0$ (on-axis field), $S(z, \rho = 0) = z$ is real. The on-axis TD field in Eq. (18) then propagates like a one-dimensional plane wave. We obtain the on-axis real stationary point, denoted $\bar{\omega}_s(\mathbf{r}, t) = \bar{\omega}_s(z, t)$, by solving

$$\frac{z}{t} = \left[\frac{\mathrm{d}k}{\mathrm{d}\omega}(\bar{\omega}_s)\right]^{-1} = v_g(\bar{\omega}_s), \tag{26}$$

where v_g is the group speed. For interpretation of this equation, see Ref. 15, Sec. 1.6, as well as Fig. 2 and Eqs. (45).

b. Off-Axis Field. For points near the beam axis, we can obtain an approximate expression for the field in Eq. (18) by expanding $\Phi(\mathbf{r}, \omega)$ in a Taylor series about the on-axis stationary point $\bar{\omega}_s$ (only the ω dependence is shown):

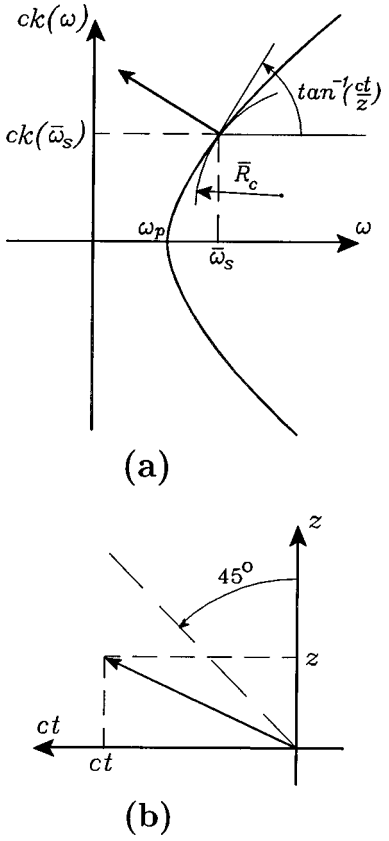

Fig. 2. On-axis PB asymptotics, dispersion surface, and space–time rays. (a) $k(\omega)$ dispersion surface. The normal to the surface [see Eqs. (45)] is parallel to the space–time ray to the observation point (z, ct). The construction determines the saddle-point values $\bar{\omega}_s(z, t)$ and $k[\bar{\omega}_s(z, t)]$. The local on-axis radius of curvature $\bar{R}_c$ of the dispersion curve is also shown [see Eq. (47)]. (b) Space–time ray to the observation point (z, ct).

$$\Phi(\omega) = \Phi_0 + \Phi_1(\omega - \bar{\omega}_s) + {}^1\!/_2\Phi_2(\omega - \bar{\omega}_s)^2, \tag{27}$$

where

$$\Phi_0 \equiv \Phi(\bar{\omega}_s) = \bar{\omega}_s t - k(\bar{\omega}_s)S(\mathbf{r}), \tag{28}$$

$$\Phi_1 \equiv \left.\frac{\partial\Phi}{\partial\omega}\right|_{\bar{\omega}_s} = t - k'(\bar{\omega}_s)S = t\left(1 - \frac{S}{z}\right), \tag{29}$$

with the prime denoting the derivative with respect to the argument. The last equality in Eq. (29) is obtained by use of Eq. (26). Φ_2 is given by

$$\Phi_2 \equiv \left.\frac{\partial^2\Phi}{\partial\omega^2}\right|_{\bar{\omega}_s} = -k''(\bar{\omega}_s)S. \tag{30}$$

Thus, from Eq. (27), the stationary point $\Phi'(\omega_s) = 0$ is seen to be

$$\omega_s = \bar{\omega}_s - \Phi_1/\Phi_2. \tag{31}$$

Choosing $\mathrm{Re}\,\bar{\omega}_s > 0$, we asymptotically evaluate the field in Eqs. (18) by the lowest-order saddle-point formula,[15]

$$\int B(\omega; \mathbf{r}, t)\exp[-i\Phi(\omega; \mathbf{r}, t)]\mathrm{d}\omega \sim \left[\frac{2\pi}{i\Phi''(\omega_s; \mathbf{r}, t)}\right]^{1/2} B(\omega_s; \mathbf{r}, t)\exp[-i\Phi(\omega_s; \mathbf{r}, t)]$$
$$\Phi'(\omega_s) = 0, \tag{32}$$

to obtain

$$\overset{+}{u}(\mathbf{r}, t) \sim A(\mathbf{r}, t)\exp[-i\Psi(\mathbf{r}, t)], \tag{33}$$

where the phase is obtained by insertion of Eq. (31) into Eq. (27):

$$\Psi(\mathbf{r}, t) \equiv \Phi(\omega_s; \mathbf{r}, t) = \Phi_0 - {}^1\!/_2\Phi_1{}^2/\Phi_2, \tag{34}$$

and the amplitude is given by

$$A(\mathbf{r}, t) = \frac{-i\beta}{z - i\beta}\hat{f}(\bar{\omega}_s)\left[\frac{-2}{\pi i k''(\bar{\omega}_s)S}\right]^{1/2}. \tag{35}$$

Recall that ω_s and $\bar{\omega}_s$ are functions of $(\mathbf{r}, t)$ and (z, t), respectively, whereas $\Phi_{0,1,2}(\mathbf{r}, \bar{\omega}_s)$ depends on $\mathbf{r}$ explicitly and on (z, t) implicitly through $\bar{\omega}_s$. Note that in Eq. (35) the amplitude is evaluated with $\bar{\omega}_s$ instead of ω_s. This approximation is based on the reasonable assumption that the deviation of the off-axis stationary point from the on-axis stationary point may be neglected in the amplitude. Also note that, in Eq. (34), the ρ dependence is not restricted to $O(\rho^2)$ and therefore goes beyond the paraxial approximation.

Stationary Frequency. In view of Eq. (31), we may write $\omega_s = \bar{\omega}_s(z, t) + \Delta_{\omega_s}(z, \rho, t)$, where Δ_{ω_s} is the deviation of the off-axis stationary frequency from the on-axis stationary frequency $\bar{\omega}_s$. Using Eqs. (28)–(30), we obtain

$$\Delta_{\omega_s}(z, \rho, t) = \frac{t\left(1 - \frac{S}{z}\right)}{k''(\bar{\omega}_s)S} = -\frac{1}{2}\rho^2\frac{1}{z - i\beta}\frac{t}{k''(\bar{\omega}_s)zS}. \tag{36}$$

From Eq. (14), we find that

$$\Delta_{\omega_s}(z,\rho,t) = -\frac{1}{2}\rho^2\frac{t}{k''(\bar{\omega}_s)z}\left\{\left(z^2 + {}^1\!/_2\,\rho^2 + \beta_i z + \frac{\beta_r{}^2 z^2}{z^2 + {}^1\!/_2\rho^2 + \beta_i z}\right)^{-1} + i\left[\beta_r z + \frac{(z^2 + {}^1\!/_2\rho^2 + \beta_i z)^2}{\beta_r z}\right]^{-1}\right\}. \tag{37}$$

Retaining the terms of $O(\rho^4)$ will facilitate estimates on the range of validity of the paraxial approximation. For $\rho \ll z$ or $\sqrt{\beta_i z}$, one may write

$$\Delta_{\omega_s}(z,\rho,t) = -\frac{1}{2}\rho^2\frac{t}{k''(\bar{\omega}_s)z}\left\{\left(z^2 + \beta_i z + \frac{\beta_r{}^2 z^2}{z^2 + \beta_i z}\right)^{-1} + i\left[\beta_r z + \frac{(z^2 + \beta_i z)^2}{\beta_r z}\right]^{-1}\right\} + O(\rho^4), \tag{38}$$

which furnishes one of the estimates.

Phase Ψ. Inserting Eqs. (28–30) into Eq. (34), we obtain

$$\Psi(z,\rho,t) = \bar{\omega}_s t - k(\bar{\omega}_s)S(z,\rho) + \frac{1}{2}t\left[1 - \frac{S(z,\rho)}{z}\right]\Delta_{\omega_s}(z,\rho,t). \tag{39}$$

Using $1 - S/z = -\rho^2/2z(z - i\beta)$ [see Eq. (13)] and expanding Ψ about the on-axis phase $\bar{\Psi} \equiv \Psi(\rho = 0)$ yields, highlighting the ρ dependence,

$$\Psi(\rho) = \bar{\Psi} + \Delta_\Psi(\rho), \tag{40}$$

where

$$\bar{\Psi} = \bar{\omega}_s t - k(\bar{\omega}_s)z,$$
$$\Delta_\Psi(\rho) = -\frac{1}{2}\rho^2\frac{1}{z(z - i\beta)}\left[\frac{1}{2}\Delta_{\omega_s}t + k(\bar{\omega}_s)z\right]. \tag{41}$$

Using Eq. (36),

$$\Delta_\Psi = \frac{1}{2}\rho^2\frac{1}{z(z - i\beta)}\left[\frac{1}{4}\rho^2\frac{1}{z - i\beta}\frac{t^2}{k''(\bar{\omega}_s)zS} - k(\bar{\omega}_s)z\right], \tag{42}$$

or

$$\Delta_\Psi = \frac{1}{2}\rho^2\frac{1}{z(z - i\beta)}\left[\frac{1}{4}\rho^2\frac{1}{z - i\beta}\frac{t^2}{k''(\bar{\omega}_s)z^2} - k(\bar{\omega}_s)z\right] + O(\rho^6), \tag{43}$$

where Eq. (43) results on Taylor expansion $(1/S)$ in ρ [see Eq. (13)].

c. Validating the Paraxial Approximation. As noted above, the expressions in Eqs. (38) and (43) include higher-order terms that are to be used to determine the range of validity of the conventional paraxial approximation. The paraxial phase is given by

$$\Psi_p(\mathbf{r},t) = \bar{\omega}_s t - k(\bar{\omega}_s)S(z,\rho), \tag{44}$$

where S is the expression in Eq. (13). Next we examine the parametric regimes for which the ρ^4 term in Eq. (43) may be neglected. To interpret the manipulations that follow, we shall anchor the parametrization to the $(ck,\ \omega)$ dispersion surface and its relation to space–time ray theory. The location of the on-axis stationary point $\bar{\omega}_s$ on the dispersion surface is found from condition (26):

$$c\left.\frac{\mathrm{d}k}{\mathrm{d}\omega}\right|_{\omega=\bar{\omega}_s} = \bar{\Omega}, \qquad \bar{\Omega} \equiv \frac{ct}{z}. \tag{45}$$

In relations (45), the nondimensional descriptor $\bar{\Omega} \geqslant 1$ parameterizes the location of an observer at z with respect to the wave front at $\bar{\Omega} = 1$, corresponding to $k(\omega) = \omega/c$. Utilizing the radius of curvature R_c of the dispersion curve, which is given by

$$R_c(\omega) = \{1 + [ck'(\omega)]^2\}^{3/2}/ck''(\omega), \tag{46}$$

yields, from Eqs. (45), the on-axis radius of curvature $\bar{R}_c$ at $\bar{\omega}_s$:

$$\bar{R}_c \equiv R_c(\bar{\omega}_s) = \frac{(1 + \bar{\Omega}^2)^{3/2}}{ck''(\bar{\omega}_s)}. \tag{47}$$

Note that R_c has the dimensionality $\omega \sim t^{-1}$ (see Fig. 2). Rewriting the phase in Eq. (39) in the form

$$\Psi = \Psi_p + \Psi_d, \tag{48}$$

where Ψ_d is the deviation of Ψ from the paraxial approximation Ψ_p in Eq. (44), and using Eq. (39), one finds that

$$\Psi_d = \frac{1}{2}t\left[1 - \frac{S(z,\rho)}{z}\right]\Delta_{\omega_s}(z,\rho,t). \tag{49}$$

Using Eqs. (38) and (13), one obtains

$$\Psi_d = \frac{1}{8}\frac{\rho^4}{(z - i\beta)^2 z^2}\frac{t^2}{zk''(\bar{\omega}_s)} + O(\rho^6). \tag{50}$$

Note that, in Eqs. (39)–(41), S is replaced by its on-axis value z and $\Delta_\Psi(\rho)$ accounts for all ρ-dependent terms, whereas, in Eqs. (48)–(50), S contains only its paraxial $O(\rho^2)$ term and Ψ_d accounts for the $O(\rho^4)$ dependence. Neglecting the ρ^6 term and using Eq. (46), one finds that

$$\Psi_d = \frac{1}{8}\frac{\rho^4}{(z - i\beta)^2 cz}\frac{\bar{\Omega}^2}{(1 + \bar{\Omega}^2)^{3/2}}\bar{R}_c. \tag{51}$$

The phase correction Ψ_d depends on the small parameter ρ/z, the on-axis observation point z, the proximity to the wave front parameterized by $\bar{\Omega}$, and the dispersion surface radius of curvature $\bar{R}_c$. Ψ_d may be neglected as long as $|\Psi_d| \ll 2\pi$, giving

$$Q_\rho \equiv \frac{1}{16\pi}\frac{\rho^4}{|z - i\beta|^2 cz}\frac{\bar{\Omega}^2}{(1 + \bar{\Omega}^2)^{3/2}}|\bar{R}_c| \ll 1, \tag{52}$$

where Q_ρ is the critical nondimensional parameter that parameterizes the maximum off-axis excursion for which the phase in Eq. (39) can be approximated by its paraxial (quadratic) form Ψ_p; i.e., the maximum off-axis excursion $\rho_{\max}$ is obtained for $Q_\rho \simeq 1$. Recall from relation (12) with Eq. (19) that, for a nondispersive field, this deviation

is parameterized by $\rho \ll z$ alone. When dispersion is introduced, the parameters $\bar{R}_c$ and $\bar{\Omega}$ play a role, in addition to z. However, the estimate in relation (52) becomes invalid when $|\bar{R}_c| \to \infty$ because Eq. (35) with Eq. (47) shows that the asymptotic field amplitude in Eq. (35) diverges in that limit.

2. $\hat{f}(\omega)$ Included in the Phase

The expression for the field in Eq. (33) is invalid when $\hat{f}(\omega)$ cannot be considered as an amplitude function. To account for the pulse beam spectrum $\hat{f}$ in Eqs. (20), one should add the term $-i\omega T/2$ to the phase and should take this term into account when performing the asymptotics. Using Eqs. (20) in Eqs. (18) yields

$$\overset{+}{u}(\mathbf{r}, t) = \frac{-i\beta}{z - i\beta} \frac{1}{\pi} \int_0^\infty d\omega \exp[-i\Phi(\omega; \mathbf{r}, t)], \quad (53)$$

$$\Phi(\omega; \mathbf{r}, t) = \omega[t - i(T/2)] - k(\omega)S(\mathbf{r}). \quad (53a)$$

From Eq. (53a), we find that the stationary frequency, ω_s satisfies

$$\frac{t - iT/2}{S} = k'(\omega_s). \quad (54)$$

Solving Eq. (54) even for on-axis observation points requires analytic continuation of the dispersion surface $ck(\omega)$ into the complex ω domain. In the following analysis we assume that both T and ρ are small parameters with respect to z and t, respectively. Performing essentially the same asymptotics as in Eqs. (27)–(35), we find that the approximated off-axis stationary frequency is given by

$$\omega_s = \bar{\omega}_s(z, t) - \frac{1}{2}\left[\frac{\rho^2 t}{z(z - i\beta)} - iT\right] \Big/ k''(\bar{\omega}_s)S \quad (55)$$

and the phase by (see Appendix A)

$$\Psi(\rho) = \bar{\omega}_s\left(t - i\frac{T}{2}\right) - k(\bar{\omega}_s)S - \frac{1}{8}\left[\frac{T^2}{k''(\bar{\omega}_s)S} + \frac{2iTt\rho^2}{z(z - i\beta)k''(\bar{\omega}_s)S}\right] + \Psi_d, \quad (56)$$

where Ψ_d, shown in Eq. (50), may be neglected subject to the condition in relation (52).

Next we determine the condition under which the two additional terms in the square brackets in Eq. (56) are negligible, so that the field may be approximated by

$$\overset{+}{u}_p(\mathbf{r}, t) = \frac{-i\beta}{z - i\beta}\left[\frac{-2}{\pi i k''(\bar{\omega}_s)S}\right]^{1/2} \exp[-i\Psi_p(\mathbf{r}, t)],$$

$$\Psi_p(\mathbf{r}, t) = \bar{\omega}_s\left(t - i\frac{T}{2}\right) - k(\bar{\omega}_s)S. \quad (57)$$

In the remainder of this section we examine in detail the critical nondimensional parameters, often referred to as numerical distances, which characterize the behavior of the PB asymptotic field [Eqs. (57)] in the dispersive environment. These critical parameters quantify not only the range of validity of Eqs. (57) but also yield measures of the resolution of various observables of the signals as a function of dispersion.

First, we note that Eqs. (57) are valid, providing

$$\frac{1}{8}\left|\frac{T^2}{k''(\bar{\omega}_s)S} + \frac{2iTt\rho^2}{z(z - i\beta)k''(\bar{\omega}_s)S}\right| \ll 2\pi. \quad (58)$$

For on-axis observation points, relation (58) yields $T^2 \ll 8\pi k''(\bar{\omega}_s)z$. Using the radius of curvature of the dispersion surface $\bar{R}_c$ in Eq. (47) yields

$$Q_T \equiv \frac{c}{16\pi z}(1 + \bar{\Omega}^2)^{-3/2}|\bar{R}_c|T^2 \ll 1, \quad (59)$$

where Q_T is the critical nondimensional parameter that bounds the maximum T for which Eqs. (57) are valid. However, as in relation (52), the estimate fails for observation points such that $\bar{R}_c \to \infty$ [see Eqs. (57)]. Combining relations (52) and (59), we define

$$Q_p \equiv Q_\rho + Q_T \simeq 1 \quad (60)$$

as the general nondimensional estimator for the paraxial approximation.

Next certain aspects of the field in Eqs. (57) can be explored by examination of the envelope of the signal. On the axis $\rho = 0$, the envelope function $E(z, t)$ is defined as

$$E(z, t) = \frac{|\beta|}{|z - i\beta|}\sqrt{\frac{2}{z\pi}} \exp[\mathrm{Im}\ \Psi(z, t)]/\sqrt{|k''(\bar{\omega}_s)|}$$
$$\propto \exp[-\bar{\omega}_s(z, t)T/2]/\sqrt{|k''(\bar{\omega}_s)|}. \quad (61)$$

Assuming that $k(\omega) \to \omega/c$ as $\omega \to \infty$, then, at the wave front, $E \to 0$ because of the dominant exponential decay. Behind the wave front, the waveform decays essentially because of the increasing $k''(\bar{\omega}_s)$.

a. On-Axis Temporal Width. For a given observation point z, the envelope peaks at time $t_{\max}$ that satisfies $dE(z, t_{\max})/dt = 0$. Using relation (61), one finds that $t_{\max}$ satisfies

$$\frac{d\bar{\omega}_s}{dt}\frac{d}{d\bar{\omega}_s}[\exp(-T\bar{\omega}_s/2)/\sqrt{k''(\bar{\omega}_s)}]\big|_{t=t_{\max}} = 0, \quad z = \text{const.}, \quad (62)$$

giving

$$[k'''(\bar{\omega}_s) + Tk''(\bar{\omega}_s)]\big|_{t=t_{\max}} = 0. \quad (63)$$

Equation (63) is first solved for $\bar{\omega}_s(z, t)$, and then $t_{\max}$ is found via Eqs. (45). The temporal width, for a given dispersion surface, may be found by use of this result with the corresponding peak value.

b. On-Axis Spatial Width. For a given observation time t, the spatial width of the field [Eqs. (57)] on the z axis is determined essentially by the second part of relation (61), i.e., by $\exp[-\bar{\omega}_s(z, t)T/2]/\sqrt{|k''(\bar{\omega}_s)|}$. Applying $d/dz = (d\bar{\omega}_s/dz)(d/d\bar{\omega}_s)$ to this expression yields that the envelope peaks at $z_{\max}$, which satisfies Eq. (63) with constant t. Therefore one uses Eq. (63) to obtain $\bar{\omega}_s$, from which $z_{\max}$ is obtained by use of Eqs. (45). The on-axis spatial width for a given dispersion surface may be found by use of this result with the corresponding peak value.

c. Off-Axis Spatial Width. The off-axis decay of the field in Eqs. (57) is determined by $\mathrm{Im}\,\Psi(\mathbf{r}, t)$. For a given on-axis space–time observation point (z, t), the field decay away from the axis is given by $\exp(\mathrm{Im}\,\Psi) \propto \exp\{-k[\bar{\omega}_s(z, t)]\rho^2/2I(z)\}$, where $I(z)$ is given in Eq. (14). Therefore the field exhibits Gaussian decay away from its on-axis peak at $\rho = 0$, and its off-axis $(1/e)$ width is given by $2\sqrt{2D}$, where

$$D(z, t) = \left\{\frac{I(z)}{k[\bar{\omega}_s(z, t)]}\right\}^{1/2}. \tag{64}$$

This result is similar to the beam width in Eq. (16) in the FD, except that here $k(\omega)$ in Eq. (16) is sampled at the on-axis stationary frequency $k(\bar{\omega}_s)$.

d. Wave-Front Radius of Curvature. The wave front associated with the signal in Eqs. (57) is characterized by the condition

$$\mathrm{Re}\,\Psi_p(\mathbf{r}, t) = \bar{\omega}_s t - k(\bar{\omega}_s)z - {}^1\!/_2 k(\bar{\omega}_s)\rho^2/R(z) = \text{const.}, \tag{65}$$

where $R(z)$ is given in Eq. (17). Equation (65) defines a surface $z = z(\rho)$, for which the wave-front radius of curvature (at $\rho = 0$) may be evaluated by the general formula in Eq. (46) with the $ck(\omega)$ surface now being replaced by the $z(\rho)$ surface. By differentiating Eq. (65) with respect to ρ and using $\mathrm{d}/\mathrm{d}\rho = (\mathrm{d}/\mathrm{d}\bar{\omega}_s)(\mathrm{d}\bar{\omega}_s/\mathrm{d}\rho)$ [recall that, in Eq. (65), z is function of ρ and that therefore $\bar{\omega}_s(z, t)$ is a function of ρ], one finds that

$$\frac{\mathrm{d}\bar{\omega}_s}{\mathrm{d}\rho}[t - k'(\bar{\omega}_s)z(\rho)] - k(\bar{\omega}_s)z'(\rho) - k(\bar{\omega}_s)\rho/R(z) + O(\rho^2) = 0. \tag{66}$$

To further simplify Eq. (66) we note, by taking the first derivative with respect to ρ of both sides of Eq. (26), that

$$\frac{\mathrm{d}\bar{\omega}_s}{\mathrm{d}\rho}[t - k'(\bar{\omega}_s)z] = 0. \tag{67}$$

Using Eq. (67) in Eq. (66), one obtains

$$-k(\bar{\omega}_s)z'(\rho) - k(\bar{\omega}_s)\rho/R(z) + O(\rho^2) = 0, \tag{68}$$

and therefore $z'(\rho)|_{\rho=0} = 0$. By taking the derivative of Eq. (67) with respect to ρ, one finds that

$$z''(\rho)|_{\rho=0} = -\frac{1}{R(z)}. \tag{69}$$

The wave-front radius of curvature may now be obtained from the general formula in Eq. (46). Inserting $z'(\rho)|_{\rho=0} = 0$ and Eq. (69) into Eq. (46), we find that the wave-front radius of curvature $R_d(z)$ for the dispersive field is given by

$$R_d(z) = -\{1 + [z'(\rho = 0)]^2\}^{3/2}[z''(\rho = 0)]^{-1} = R(z), \tag{70}$$

where $R(z)$ is as defined in Eq. (17). Note that the minus sign in Eq. (70) was chosen in accordance with the convention that the wave-front radius of curvature is positive for a diverging wave front [see also Eq. (17)]. From the discussion that follows Eq. (22), the wave-front radius of curvature in the near-wave-front field is also given by $R(z)$. Dispersion does not affect this result [even when the additional ρ^4 term in Eq. (43) is taken into account] because the beam field is isodiffracting with frequency-independent radius of curvature of the corresponding FD field [see Eq. (17)].

e. Instantaneous Frequency. The instantaneous frequency $\omega_i(\mathbf{r}, t)$ may be evaluated by means of $\omega_i = \mathrm{Re}\,\mathrm{d}\Psi_p/\mathrm{d}t$, where Ψ_p is given as in Eqs. (57). Taking the first derivative of $\mathrm{Re}\,\Psi_p$ with respect to t and using Eq. (14), one obtains

$$\omega_i = \bar{\omega}_s + \frac{\mathrm{d}\bar{\omega}_s}{\mathrm{d}t}[t - k'(\bar{\omega}_s)z] - \frac{\mathrm{d}\bar{\omega}_s}{\mathrm{d}t}k'(\bar{\omega}_s)\frac{{}^1\!/_2\rho^2}{R(z)} = \bar{\omega}_s - \frac{\mathrm{d}\bar{\omega}_s}{\mathrm{d}t}\frac{t}{z}\frac{{}^1\!/_2\rho^2}{R(z)}, \tag{71}$$

where $R(z)$ is given by Eq. (17) and the last equality is obtained by use of Eq. (26). Taking the first derivative of Eq. (26) with respect to time, one finds that $\mathrm{d}\bar{\omega}_s/\mathrm{d}t = [k''(\bar{\omega}_s)z]^{-1}$, and Eq. (71) yields

$$\omega_i(\mathbf{r}, t) = \bar{\omega}_s(z, t) - \frac{t}{z^2 k''(\bar{\omega}_s)}\frac{\rho^2/2}{R(z)}. \tag{72}$$

To relate this result to local geometrical properties of the dispersion surface $ck(\omega)$, we insert Eq. (47) into Eq. (72), which gives

$$\omega_i(\mathbf{r}, t) = \bar{\omega}_s(z, t) - \frac{1}{2}\rho^2\frac{\bar{R}_c}{zR(z)}\frac{\bar{\Omega}}{(1 + \bar{\Omega}^2)^{3/2}}, \qquad \bar{\Omega} \equiv \frac{ct}{z}. \tag{73}$$

Thus the on-axis instantaneous frequency due to dispersion is given by the on-axis stationary frequency $\bar{\omega}_s$. The deviation of ω_i from this frequency for off-axis observation points is proportional to ρ^2 times the ratio between the dispersion surface radius of curvature $\bar{R}_c$ and the wave-front radius of curvature $R(z)$.

5. CONCLUSION

In this paper we have been concerned with the parameterization of the effects of frequency dispersion on the propagation characteristics of a paraxially approximated pulsed beam (PB) wave packet in a lossless medium with generic wave-number profile $k(\omega)$. Various nondimensional measures—critical parameters—have been defined to systematically assess and quantify (a) the effect of dispersion on various observables associated with the PB field and thereby on the resolution of these observables, and (b) the range of validity of the paraxial approximation under these conditions. Relating the critical parameters to space–time ray theory and wave-number–frequency dispersion surfaces has further elucidated the relevant wave dynamics. Refinement of these results for the nondispersive-to-dispersive transition regime, as well as specific calculations for a simple Lorentz medium, are contained in a companion paper,[16] in which we assess the accuracy of the critical parameters.

APPENDIX A: DERIVATION OF EQS. (55) AND (56)

To derive the PB asymptotics when the term $\exp(-\omega T/2)$ is included in the phase, we expand $\Phi(\omega)$ into a Taylor series about the on-axis stationary point $\bar{\omega}_s$ as in Eq. (27), where $\bar{\omega}_s$ is defined as above by Eq. (26). Using Φ in Eq. (53a), we obtain [cf. Eq. (28)–(30)]

$$\Phi_0 = \bar{\omega}_s[t - (i/2)T] - k(\bar{\omega}_s)S(\mathbf{r}), \tag{A1}$$

$$\Phi_1 = t[1 - (S/z)] - (i/2)T, \tag{A2}$$

with Φ_2 being given by Eq. (30). Using Eqs. (A1), (A2), and (30) in Eqs. (31) and (34), we obtain the final results in Eqs. (55) and (56), respectively.

ACKNOWLEDGMENTS

This research was supported in part by the Naval Coastal Systems Center, Panama City, Florida, under Office of Naval Research grant N61331-96-K-0028. Also, T. Melamed acknowledges partial support from a 1996–97 Dean's Postdoctoral Fellowship at Boston University, and L. B. Felsen acknowledges partial sponsorship under U.S.–Israel Binational Science Foundation grant 95-00399.

*Also with Department of Electrical and Computer Engineering, Boston University, Boston, Massachusetts 02215.

REFERENCES

1. K. A. Connor and L. B. Felsen, "Gaussian pulses as complex-source-point solutions in dispersive media," Proc. IEEE **62**, 1614–1615 (1974).
2. K. E. Oughstun and G. C. Sherman, *Electromagnetic Pulse Propagation in Causal Dielectrics*, Vol. 16 of Springer Series on Wave Phenomena (Springer, New York, 1997).
3. K. E. Oughstun, "Dynamical structure of the precursor fields in linear dispersive pulse propagation in lossy dielectrics," *Ultra-Wideband, Short-Pulse Electromagnetics 2*, L. Carin and L. B. Felsen, eds. (Plenum, New York, 1995), pp. 257–272.
4. C. M. Balictsis and K. E. Oughstun, "Uniform asymptotic description of Gaussian pulse propagation of arbitrary initial pulse width in a linear, causally dispersive medium," in *Ultra-Wideband, Short-Pulse Electromagnetics 2*, L. Carin and L. B. Felsen, eds. (Plenum, New York, 1995), pp. 273–283.
5. J. G. Blaschak and J. Franzen, "Precursor propagation in dispersive media from short-rise-time pulses at oblique incidence," J. Opt. Soc. Am. A **12**, 1501–1512 (1995).
6. P. G. Petropoulos, "Wave hierarchies for propagation in dispersive electromagnetic media," in *Ultra-Wideband, Short-Pulse Electromagnetics 2*, L. Carin and L. B. Felsen, eds. (Plenum, New York, 1995), pp. 351–354.
7. B. Z. Steinberg, E. Heyman, and L. B. Felsen, "Phase-space beam summation for time-dependent radiation from large apertures: continuous parameterization," J. Opt. Soc. Am. A **8**, 943–958 (1991).
8. T. Melamed, "Phase-space beam summation: a local spectrum analysis for time-dependent radiation," J. Electromagn. Waves Appl. **11**, 739–773 (1997).
9. E. Heyman and L. B. Felsen, "Complex source pulsed beam fields," J. Opt. Soc. Am. A **6**, 806–817 (1989).
10. E. Heyman, "Pulsed beam propagation in an inhomogeneous medium," IEEE Trans. Antennas Propag. **42**, 311–319 (1994).
11. T. Melamed and E. Heyman, "Spectral analysis of time-domain diffraction tomography," invited paper for the special issue on the International Union of Radio Science 1995 Electromagnetic Theory Symposium, Radio Sci. **32**, 593–604 (1997).
12. T. Melamed, E. Heyman, and L. B. Felsen, "Local spectral analysis of short-pulse-excited scattering from weakly inhomogeneous media: Part I. Forward scattering," Department of Aerospace and Mechanical Engineering, Boston University, Boston, Mass. 02215, Rep. No. AM-97-023, 1997.
13. T. Melamed, E. Heyman, and L. B. Felsen, "Local spectral analysis of short-pulse-excited scattering from weakly inhomogeneous media: Part II. Inverse scattering," Department of Aerospace and Mechanical Engineering, Boston University, Boston, Mass. 02215, Rep. No. AM-97-024, 1997.
14. E. Heyman and T. Melamed, "Certain considerations in aperture synthesis of ultrawideband/short-pulse radiation," IEEE Trans. Antennas Propag. **42**, 518–525 (1994).
15. L. B. Felsen and N. Marcuvitz, *Radiation and Scattering of Waves* (IEEE, Piscataway, N.J., 1994). Classic reissue.
16. T. Melamed and L. B. Felsen, "Pulsed-beam propagation in lossless dispersive media. II. Applications," J. Opt. Soc. Am. A **15**, 1277–1284 (1998).